Published in final edited form as:
Pain. 2010 February ; 148(2): 237–246. doi:10.1016/j.pain.2009.11.003.

N-Methyl-D-Aspartate Receptor (NMDAR) independent maintenance of inflammatory pain

Amanda R. Weyerbacher[1], **Qinghao Xu**[1,2], **Cristina Tamasdan**[3], **Sarah J. Shin**[1], and **Charles E. Inturrisi**[1,3,*]

[1]Department of Pharmacology, Weill Cornell Medical College, New York, NY 10065

[3]Department of Neurology and the Pain and Palliative Care Service, Memorial Sloan-Kettering Cancer Center, 1275 York Ave. New York, NY 10065, USA

Six key words

NMDA receptor; ERK2; astrocytes; interleukin-1β; inflammatory pain; spinal cord dorsal horn

1. Introduction

Peripheral inflammatory mediators sensitize and activate high threshold primary sensory neurons and this activity is conducted to central terminals that synapse on second order neurons in the spinal cord dorsal horn (SCDH). With the intense and sustained noxious stimuli that are associated with persistent inflammation, there is a temporal summation of postsynaptic depolarizations, which removes the voltage-dependent magnesium block of N-Methyl-D-Aspartate receptors (NMDAR) allowing calcium influx into the postsynaptic cell. This in turn activates calcium sensitive intracellular signal cascades that lead to rapid posttranscriptional changes such as the phosphorylation of the NR1 subunit of the NMDAR, the Kv4.2 potassium channel, [11], protein kinase C (pPKC) and extracellular signal-regulated kinases, ERK1 and ERK2 (pERK1/2) [14-16]. These and other phosphorylated kinases can initiate events that lead to a later, sustained transcription of genes associated with pain such as COX-2, TrkB and BDNF [15]. The resulting prolonged increase in the excitability of spinal cord neurons and the recruitment of normally subliminal inputs leads to the spread of pain sensitivity beyond the site of inflammation (secondary hyperalgesia) and the generation of pain in response to low threshold inputs (allodynia). This process is described as central sensitization [34;35].

It is now well recognized that spinal glia (both microglia and astrocytes) are key contributors to persistent pain. Glia are activated by the neuronal excitation that occurs with inflammation, and in turn release proinflammatory cytokines that modulate neuronal excitability. The reciprocal interactions between neurons and glia amplify neuronal input, facilitating the maintenance of injury-induced pain [25]. However, the neuron-glia signaling mechanisms involved in the initiation and maintenance of inflammatory pain are just beginning to emerge.

*Corresponding Author: Dr. Charles E. Inturrisi, Department of Pharmacology, Weill Cornell Medical College, 1300 York Avenue, Room LC-524, New York, NY 10065, Phone: 212-746-6235, Fax: 212-746-8835, ceintur@med.cornell.edu.
[2]present address: Anesthesia Research Laboratory, 9500 Gilman Drive (CTF C-312), La Jolla, CA 92093-0818

In previous studies, we have selectively targeted the functionally essential NR1 subunit of the NMDAR in the SCDH in vivo using the serotype-2AAV vector. This vector selectively transduces neurons in vivo with vector-induced GFP expression confined to NeuN-positive cells and absent from glia (GFAP- positive cells) [17]. This neurotropic vector has been used to produce a spatial NMDAR knockout (NR1 KO) [29] and an siRNA knockdown (KD) [6; 7]. Together with an antisense mediated knockdown of NR1[28], these studies provide converging evidence that postsynaptic NMDARs in the SCDH are required for the central sensitization resulting from peripheral inflammation. We also observed that the NR1 KO does not provide sustained protection against inflammatory pain [19]. In contrast, an siRNA targeting the expression of neuronal ERK2 in the SCDH prevents thermal and mechanical pain for up to 96 hr after CFA-induced peripheral inflammation (Xu et al., 2008). In the present report we extend these observations so as to more precisely define the neuronal and glial signaling mechanisms that contribute to inflammation-induced pain hypersensitivity.

2. Methods

2.1 Experimental animals and drugs

Adult mice (8-12 weeks) homozygous for the floxed NR1 subunit (fNR1) gene [29] of both sexes were used for this study. The NR1 floxed mice have a C57BL/6 background [29]. Experiments were performed in accordance with National Institutes of Health Guidelines for the Care and Use of Laboratory Animals. The experimental protocol [9-772A] was approved by the Institutional Animal Care and Use Committee at Weill Cornell Medical College. Animals were housed under 12 hr light/dark cycles in a pathogen-free room with free access to water and food.

2.2 Intraparenchymal injection of the rAAV vectors

To produce a spatial NR1 knockout (NR1 KO), the rAAV vector expressing green fluorescent protein (GFP) and Cre recombinase was microinjected into the right (ipsilateral) spinal cord dorsal horn (SCDH) as described by South et al. [29]. Vector controls received rAAV-GFP, a vector that lacks the coding sequence for CRE recombinase. The mice were anesthetized with ketamine/xylazine and a laminectomy was performed to remove part of the dorsal L2 and L3 spinous process and the lumbar area of the spinal cord was exposed for intraparenchymal injection (IPI). Three unilateral injections of 1 μl (2×10^9 viral particles/μl) were administered 0.5-0.7 mm apart, at a depth of 0.3 mm from the dorsal border and 0.5 mm from the midline, using a glass pipette with a 40-μm-diameter tip attached to a 5 μl Hamilton syringe. The syringe was mounted on a microinjector (David Kopf Instruments, Tujunga, CA) attached to a stereotaxic unit (David Kopf Instruments). After the injection, the overlying muscles were closed with 5-0 chromic gut and the skins were closed with wound clips. Animals were allowed to recover for two weeks before undergoing behavioral tests, or sacrificed for histological and Western blot analysis. The same IPI procedure with an rAAV vector that expressed GFP and an ERK2 siRNA was used to produce the spatial KD of ERK2 in the SCDH [36].

2.3 Immunoblot

Animals were deeply anesthetized by isoflurane, decapitated and the lumbar spinal cords at the level of L4-L6 were rapidly dissected. The right and left spinal cords were separated and immediately homogenized in modified RIPA buffer (50mM Tris-HCl, pH7.4, 1% NP40, 1mM EDTA, 150mM NaCl) supplemented with protease inhibitor cocktail (Sigma) diluted 1:10, 2mM PMSF, 2mM NaF and phosphatase inhibitor cocktail I and II (Sigma), then frozen in liquid nitrogen. After all the samples were collected, tissues were thawed on ice, sonicated and centrifuged at 4°C at 14000g for 10 min to obtain the supernatant. The protein level of each sample was measured by the BioRad DC assay. Samples were then diluted in Laemmli sample

buffer on the same day to a final concentration of 2 ug/ul, boiled for 5 min and stored at -80° C.

The spinal cord samples were separated on SDS-PAGE gels (10% Tris-HCl gel; Bio-Rad, Hercules, CA) and transferred to polyvinylidene difluoride filters (PVDF, Millipore, Bedford, MA), which were subsequently blocked in blocking solution (5% dry milk in TBS with 0.1% Tween-20) for at least an hour. Membranes were incubated with rabbit anti-phospho-ERK1/2 (pERK1/2) antibody (1:1000; Cell Signaling Technology, Inc.) or rabbit anti-phospho PKCγ (pPKCγ) antibody (1:500; Cell Signaling) in blocking solution overnight at 4°C, washed in TBS with 0.1% Tween-20 (TBST), then incubated with HRP-conjugated anti-rabbit IgG (1:1000, Pierce Biotechnology, Inc., Rockford, IL) in blocking solution for 1 hr. Membranes were washed with TBST followed by TBS and developed using SuperSignal West Pico ECL kit (Pierce Biotechnology, Inc.), then exposed to film (Kodak, Rochester, NY) for various times. Next, membranes were stripped (Pierce) and reprobed for ERK1/2 using rabbit anti-ERK1/2 antibody (1:5000, Cell Signaling Technology, Inc.) followed by HRP-conjugated anti-rabbit secondary antibody (1:10,000, Pierce Biotechnology, Inc.). For loading control, blots were further stripped and re-probed for β–actin using a mouse monoclonal antibody (1:50,000, Sigma) followed by HRP-conjugated anti-mouse secondary antibody (1:200,000, Pierce Biotechnology, Inc.). Exposures yielding signal intensity in the linear range without saturation were used for densitometry analysis with Fluorchem 9900 (Alpha Innotech, San Leandro, CA). Ratios of intensity of pERK1/2 or pPKCγ to β–actin were calculated, normalized to the intensity of the control samples on the same blot and subjected to statistical analysis. At least 3 animals were included in each treatment group.

2.4 Immunohistochemistry (IHC)

Mice were anesthetized with pentobarbital and then perfused transcardially with 4% paraformaldehyde (PFA). The spinal cord was dissected and placed in 4% PFA for 1 hr before being transferred to 30% sucrose for cryoprotection for 72 hr. Lumbar spinal cord cryosections of 20-μm thick were obtained from a cryostat (Leica, Bannockburn, IL) for IHC. Spinal cord sections were incubated in blocking solution (3% normal goat serum, 0.1% Triton X-100 in Tris buffered saline) for 30 min. After washing in Tris buffered saline (TBS), sections were incubated with one or two of the following primary antibodies: rabbit anti-GFP (1:1000; Invitrogen-Molecular Probes Inc, Eugene, OR), rabbit anti-phospho-ERK1/2 (1:1000; Cell Signaling Technology, Inc., Danvers, MA), rat anti-interleukin-1β (1:50; Endogen, Rockford, IL), rabbit anti-interleukin-1 receptor (1:500; Santa Cruz), mouse anti-NeuN (1:400; Millipore-Chemicon, Bedford, MA), mouse anti-GFAP (1:2000; Millipore-Chemicon) and rat anti-OX42 (1:100, BD Biosciences, San Diego, CA) overnight in blocking solution at 4°C. The sections were washed in TBS and then incubated in appropriate fluorescent secondary antibodies or biotinylated goat anti-rabbit (1:250; Vector Laboratories, Burlingame, CA) in blocking solution. Slides were mounted in the anti-fading mounting medium GelMount (Invitrogen, Eugene, OR). A negative control was performed using diluted normal goat serum instead of the primary antibody.

2.5 Microscopic analysis

Fluorescent IHC images were captured by a Zeiss LSM 510 laser scanning confocal microscope. Quantitative analysis of IL-1β immunolabeling was performed by a blinded observer using Metamorph software (Universal Imaging, Downingtown, PA). Briefly, a threshold signal limited exclusively to those that were of a specific intensity was set as a constant within a designated region of the SCDH. The thresholded area of labeling was normalized to the total area of the region to yield a percentage thresholded area. A total of 4-5 sections spacing 400-500 μm apart were used for each animal. At least three animals were included in each treatment group.

2.6 Behavioral testing

All behavioral testing was conducted by a blinded observer. Mechanical stimulus threshold to a non-noxious mechanical stimulus was determined by paw withdrawal to the application of a series of calibrated von Frey filaments to the surface of the hind paws. The animals were placed in an open top Plexiglas cage (3.25 wide × 9 inches high) with mesh flooring that was suspended above the researcher and left to acclimate for 30 min. von Frey filaments were applied perpendicularly against the mid-plantar surface of the foot. The “up-down” method of Dixon [2] was used to determine the value at which paw withdrawal occurred 50% of the time, interpreted as the mechanical threshold.

Fifteen μl of CFA (1mg/ml *Mycobacterium tuberculosis*; Sigma) was injected into the right hind paws of lightly restrained mice. The mice had received no IPI, IPI of a rAAV-GFP vector, or IPI of a rAAV-GFP-CRE vector in the right (ipsilateral) SCDH at least two weeks prior to the intraplantar injection of CFA. Mechanical stimulus threshold and paw size using calipers were measured before (baseline) and at 24, 48 and 96 hr after CFA.

In a separate experiment, three groups of mice (fNR1, vector controls and NR1 KO) received intraplantar injections of CFA. Mechanical stimulus threshold was measured before (baseline) and at 24, 48 and 96 hr after CFA. Following the measurement of the mechanical stimulus threshold at 96 hr after CFA, vector control and NR1 KO mice received an intrathecal injection of the human IL-1 receptor antagonist (IL-1ra) (Amgen, Thousand Oaks, CA) at 10μg/5μl/mouse as described previously [12]. An additional group of fNR1 mice that did not receive IPI treatment were intrathecally injected with the IL-1ra placebo solution (Amgen) which served as a control. Thirty minutes after the intrathecal administration of either IL-1ra or placebo, behavioral testing was repeated.

A separate group of fNR1 mice received intraplantar CFA (but not IPI) and the mechanical stimulus threshold was measured at 24, 48 and 96 hr after CFA. Immediately after measuring the mechanical threshold at 24, 48 and 96 hr after CFA, the competitive NMDAR antagonist, (-)-6-phosphono-methyl-deca-hydroisoquinoline-3-carboxylic acid (LY235959), provided by Lilly Research Laboratories (Indianapolis, IN) was injected intrathecally at 75pmol/5μl/mouse at the L5-L6 intravertebral space as described previously [12]. A separate group of fNR1 mice received intraplantar CFA (but not IPI) and mechanical stimulus threshold was measured at 24, 48 and 96 hr after CFA, immediately followed by intrathecal saline at 24, 48 and 96 hr after CFA. Thirty minutes after the intrathecal injection of LY235959 or saline, the measurement of mechanical threshold was repeated. All drugs were dissolved in sterile saline and injected at a volume of 5μl.

2.7 Statistical analysis

The behavioral and Western blot data were analyzed by one-way ANOVA followed by the Student-Newman-Keuls test (multiple groups) or the t test (two groups) using the InStat software (GraphPad, version 3.00, San Diego, CA). The data are represented as mean±SEM.

3. Results

3.1 Effects of a spatial (spatiotemporal) knock-out of the NR1 subunit on CFA-induced nociception (pain hypersensitivity)

Two weeks after IPI, paw size and mechanical thresholds were measured and served as baseline comparisons before CFA injection (Fig. 1A and B). The spatial KO of NR1 was performed by IPI of the rAAV-GFP-CRE vector into the right (ipsilateral) side of the SCDH of adult NR1 floxed (fNR1) mice. For the vector control group, the rAAV-GFP vector was used for IPI. After intraplantar CFA administration, there was an equal increase in paw size in both vector

control and NR1 KO mice (Fig. 1A, $p<0.05$ vs. baseline, n=16 per treatment group), indicating a similar degree of peripheral inflammation. However, only mice in the vector control group exhibited significant decreases in the mechanical withdrawal threshold (mechanical allodynia) (Fig. 1B, $p<0.05$) at 24, 48 and 96 hr after CFA. NR1 KO mice were protected from developing mechanical allodynia at 24 hr and 48 hr, but not at 96 hr after CFA (Fig. 1B, $p<0.05$). In a separate experiment, the intrathecal administration of LY235959 (LY; 75pmol/5 μl/mouse), an NMDAR antagonist, in fNR1 mice reversed CFA-induced mechanical allodynia at 24 hr and 48 hr, but not at 96 hr after CFA. Intrathecal saline had no effect on CFA-induced mechanical allodynia (supplemental Fig.1). The increase in the mechanical threshold in response to LY seen at 24 hr after CFA appears to be an antinociceptive response. Nevertheless, the next dose at 48 hr was antiallodynic and by 96 hr LY was unable to alter the allodynic effect of CFA.

3.2 Effects of the NR1 KO on PKCγ activation in the ipsilateral lumbar spinal cord after intraplantar CFA administration

To investigate the signaling cascades underlying the development and maintenance of CFA-induced pain hypersensitivity, we examined the expression of phospho-PKCγ (pPKCγ). As shown in Figure 2, Western blot analysis demonstrates minimal pPKCγ expression in the ipsilateral spinal cord in sections of both vector control and NR1 KO mice in the absence of intraplantar CFA (No Treatment, NT). There was a significant increase in pPKCγ expression in the ipsilateral lumbar spinal cord at 24 hr after CFA in vector control sections which persisted for up to 96 hr when compared to sections of mice that did not receive intraplantar CFA (Fig 2B, $p<0.05$). However, while this significant increase in pPKCγ expression was attenuated in sections of the NR1 KO at 24 hr after CFA, pPKCγ expression was equivalently increased in sections of both vector control and NR1 KO mice at 96 hr after CFA.

3.3 Effects of NR1 KO on ERK2 activation in the ipsilateral lumbar spinal cord after intraplantar CFA administration

Western blot analysis demonstrates minimal pERK2 expression in the ipsilateral spinal cord in sections of both vector control and NR1 KO mice in the absence of intraplantar CFA (NT) (Fig 3A and B). There was a significant increase in pERK2 expression in the ipsilateral lumbar spinal cord at 24 hr after CFA in vector control sections, which persisted for up to 96 hr when compared to sections of mice that did not receive intraplantar CFA (NT) (Fig. 3A and B, $p<0.05$). However, while this significant increase in pERK2 expression in the ipsilateral lumbar spinal cord was attenuated in sections of the NR1 KO at 24 hr after CFA, pERK2 expression was equivalently increased in sections of both vector control and NR1 KO mice at 96 hr after CFA. pERK1 expression was more variable and not significantly increased ($p>0.05$) after CFA in the ipsilateral lumbar spinal cord in sections of both vector control and NR1 KO mice when compared to sections of mice that did not receive intraplantar CFA (NT) (Fig 3A and C). There were no changes in total ERK1 or ERK2 expression (data not shown).

3.4 Inflammation induces an increase in pERK2 in the SCDH in different cell types

While PKCγ expression is restricted to SCDH neurons [3], activation of both neuronal and glial pERK1/2 has been implicated in injury-induced pain (reviewed by Ji et al., 2008). Therefore, we examined the cellular localization of pERK1/2 after intraplantar CFA on spinal sections with immunohistochemistry (IHC). Because of the high sequence similarity between the ERK1 and ERK2 proteins and the lack of a specific ERK2 antiserum, IHC is unable to distinguish ERK1 and ERK2. However, the pERK1/2 immunolabeling that we examined in our model of inflammatory pain is a representation of mainly pERK2, based on the unaltered pERK1 expression in Western blot analysis (Fig. 3A and C) and our previous findings which

showed that selective inhibition of only ERK2 in the mouse SCDH resulted in a decrease in pERK1/2 immunolabeling [36].

In the present study, pERK1/2 immunolabeling was observed in the lumbar ipsilateral SCDH in sections of vector control mice, mainly in lamina I and II at 24 hr after CFA (Fig. 4A). Confocal double fluorescent IHC revealed that pERK1/2 immunolabeling was colocalized with NeuN, a neuronal marker (Fig. 4A-C) but not with GFAP, a marker of activated astrocytes (Fig. 4D) or OX42, a microglia marker (Fig 4E). However, consistent with the Western blot analysis (Fig. 3B), pERK1/2 immunolabeling was attenuated in the ipsilateral SCDH in sections of NR1 KO animals at 24 hr after CFA (Fig. 4F) when compared to sections of vector control mice (Fig. 4A). In addition, we did not observe colocalization of pERK1/2 with NeuN (Fig. 4F-H), GFAP (Fig. 4I) or OX42 (Fig. 4J) in spinal sections of NR1 KO mice at 24 hr after CFA.

The morphology of pERK1/2 at 96 hr after CFA in spinal sections of the vector control (Fig. 5A) appears different when compared to spinal sections at 24 hr after CFA (Fig. 4A). At 96 hr after CFA, pERK1/2 colocalizes with GFAP (Fig. 5A-C) but not NeuN or OX42 (Fig. 5D,E). Consistent with Western blot analysis, we observed pERK1/2 immunolabeling in spinal sections of NR1 KO mice at 96 hr after CFA. Similar to vector control sections, pERK1/2 in NR1 KO sections also colocalizes with GFAP (Fig. 5F-H) but not NeuN (Fig. 5I) or OX42 (Fig. 5J). Examination at a higher magnification supported these observations (data not shown).

Furthermore, at 96 hr after CFA, the morphology of GFAP immunolabeling in both vector control (Fig. 5B) and NR1 KO (Fig. 5G) sections exhibited hypertrophy and extended processes, that are not observed with GFAP immunolabeling at 24 hr after CFA (Fig. 4D,I).

3.5 Inflammation induces an increase in the proinflammatory cytokine IL-1β in astrocytes

We examined IL-1β expression in the ipsilateral SCDH and found minimal immunolabeling in spinal sections of both vector control (Fig. 6A) and NR1 KO mice (data not shown) in the absence of CFA (NT). At 24 hr after CFA, we observed a slight increase in IL-1β immunolabeling in spinal sections of both vector control (Fig. 6B) and NR1 KO mice (Fig. 6C). The antibody used in these studies would be expected to also detect the proIL1-β form, so that the observed immunolabeling could represent expression of the precursor as well as the mature Il-1β. Nevertheless, when we quantified IL-1β immunolabeling as a percentage of threshold in a designated area of the SCDH, it was not significantly different at 24 hr after CFA in vector control or NR1 KO mice compared to IL-1β immunolabeling in mice that did not receive CFA (NT) (Fig. 6G). However, at 96 hr after CFA, we observed an equivalent increase in IL-1β immunolabeling in sections of both vector control (Fig. 6D) and NR1 KO (Fig. 6E) mice, which was significant when compared to the absence of CFA and 24 hr after CFA (Fig. 6G). Double labeling immunofluorescence in the SCDH of both vector control and NR1 KO sections revealed that IL-1β colocalized with GFAP (Fig. 7), but not with NeuN or OX42 (data not shown). We also examined IL-1β expression in the SCDH in sections of mice with a selective knockdown of ERK2 after IPI of a vector expressing an ERK2 siRNA. In these sections, we found that the CFA-induced increase in IL-1β in the SCDH of both vector control and NR1 KO mice was completely prevented (Fig. 6F,G).

3.6 Intrathecal administration of the IL-1 receptor antagonist reverses CFA-induced persistent mechanical allodynia

We studied the effects of IL-1 signaling by blocking the IL-1 receptor with an antagonist, IL-1ra, in persistent CFA-induced mechanical allodynia at 96 hr in vector control and NR1 KO mice. Consistent with the data presented in Figure 1, mechanical withdrawal thresholds were equivalent in both groups before intraplantar CFA (baseline; Fig. 8). However, vector

control mice exhibited significant decreases in the mechanical withdrawal threshold at 24, 48 and 96 hr after CFA. NR1 KO mice were protected from mechanical allodynia at 24 and at 48 hr after CFA, but this protection was lost by 96 hr after CFA. Intrathecal administration of IL-1ra (10 mg/5 ml/mouse) at 96 hr after CFA reversed mechanical allodynia in both vector control and NR1 KO mice. To ensure the observer conducting the behavioral testing was blinded, a separate group of fNR1 mice not given IPI received intrathecal administration of a placebo drug at 96 hr after CFA. These animals exhibited mechanical allodynia at 24, 48 and 96 hr after CFA, but intrathecal administration of the placebo drug had no effect on mechanical withdrawal thresholds. Our immunolabeling experiments showed that the IL-1 receptor (IL-1R) in the SCDH colocalized with neurons, but not microglia or astrocytes at 96 hr after CFA in the SCDH of Vector Control animals (Supplemental Figure 2). We also observed the same neuronal localization of IL-1R in SCDH from NR1KO and Vector Control animals at 24 hr after CFA or no treatment (data not shown)

4. Discussion

We demonstrate that the allodynic hypersensitivity that occurs after peripheral inflammation exhibits the well established NMDAR dependence, followed by a newly characterized NMDAR-independent component. In addition, we show that the initial increase in the expression of neuronal pERK2 followed by astrocytic pERK2 in the SCDH is required for the manifestation of these temporal components of inflammatory pain (allodynia). Lastly, we show that the late occurring or NMDAR-independent maintenance phase of inflammatory pain requires the ERK2 dependent expression of the proinflammatory cytokine, IL-1β, in SCDH astrocytes. In previous studies we have provided a detailed description of the anatomical, electrophysiological and behavioral consequences of the spatial KO of NR1 [29] and the siRNA mediated KD of the expression of ERK2 [36].

The Cre-LoxP method used to produce the NR1KO results in a permanent somatic mutation of the NR1 subunit gene without loss or damage to vector transduced neurons or evidence of glia activation [29]. We found that the NR1 KO does not affect baseline mechanical thresholds in the absence of an injury-inducing stimulus. However, in a persistent inflammatory pain model evoked by intraplantar CFA, NR1 KO mice were protected from CFA-induced mechanical allodynia at 24 hr and at 48 hr after CFA. This protection was lost by 96 hr after CFA and mechanical allodynia in the NR1 KO was equivalent to that of vector control mice that express fully functional NMDARs. This transient attenuation of CFA-induced allodynia in the NR1 KO was also observed by blocking spinal NMDARs with intrathecal administration of the NMDAR antagonist, LY235959. This pharmacological antagonism reversed CFA-induced mechanical allodynia at 24 hr and at 48 hr, but not at 96 hr after CFA. In a previous report, we showed that the protection of the NR1 KO was lost by 48 hr after CFA. This study employed a different dose of CFA and that may account for the temporal difference in the loss of protection compared to the results in Figure 1. However, we consistently observe a loss of antiallodynic efficacy with either the spatial knockout (an absence of receptor function) or a pharmacological antagonist (an intermittent blockade of receptor function). Taken together, these results indicate that the ability of NMDARs to mediate inflammatory pain hypersensitivity is temporally dependent.

The NR1 KO provides the opportunity to examine the signaling pathways that are initiated following NMDAR activation. Although multiple signaling pathways are also involved, [12; 18;19;33], NMDARs play a major role in ERK1/2 activation in SCDH neurons [3;13]. However, prior studies have followed ERK activation only to 48hr after CFA and measured the expression of pERK1/2 but not each isoform. We did not detect changes in pERK1 expression after CFA in either vector control or NR1 KO mice. Rather, the increase at 24 hr after CFA was limited to pERK2 expression in the SCDH of vector control mice that was

restricted to neurons and did not occur in microglia or astrocytes. Previously, we have reported that the selective KD of ERK2 gene expression in SCDH neurons also prevents both the CFA-induced induction of pERK2 and mechanical allodynia at 24 hr after CFA [36]. Thus, either a loss of functional NMDARs or the direct reduction of ERK2 has the same behavioral and biochemical consequences. These results indicate that the early phase (24 hr) of CFA-induced pain hypersensitivity is a result of NMDAR mediated activation of neuronal pERK2 expression.

At 96 hr after CFA a different picture emerges. The NR1 KO no longer provides protection from allodynia and the expression of pERK2 in the SCDH of these mice is no longer suppressed but rather is now expressed predominately in spinal astrocytes as compared to neurons or microglia. Thus, pERK2 can be activated in astrocytes in the absence of the NMDAR. The results of our previous study [36] indicate that the KD of ERK2 by a neurotropic vector that delivered an ERK2 siRNA only to neurons is sufficient to provide both complete protection from persistent inflammatory pain and prevents neuronal and glial ERK2 expression in SCDH.

Therefore, the activation of astrocytic pERK2 that is sufficient to produce inflammatory allodynia reported in the present findings requires prior expression of pERK2 in neurons. Consistent with these observations, we also noted that CFA induced astroglial proliferation at 96 hr, which is characterized by an increase in GFAP expression, hypertrophy and thickenening of processes [1]. These changes were not observed in astrocytes at 24 hr after CFA. This activation of astrocytes may result from the ability of pERK2 to induce cellular proliferation [23].

Next, we considered neuronal kinases that can operate at least in part in the absence of the NMDAR. PKCγ is dependent on intracellular calcium and has been implicated in CFA-induced pain hypersensitivity [3;8;30]. PKCγ expression is restricted to neurons in the inner lamina II of the SCDH and pPKCγ can activate ERK1/2 [18;19;26]. CFA induced an increase in pPKCγ expression in the ipsilateral spinal cord of vector control mice at 24 and 96 hr after CFA. In contrast, the CFA induced increase in pPKCγ expression was seen at 96 hr but not at 24 hr after CFA in the NR1 KO. These data suggest, but do not prove, that neuronal PKCγ expression in the NR1 KO mice between 24 and 96 hr after CFA may be one of the triggers in neuronal signaling that activates astrocytic pERK2.

Although we did not determine how neurons signal to astrocytes, a noxious stimulus in the periphery releases glutamate, ATP and substance P which activate receptors expressed in astrocytes [25]. Ultimately, pERK2 or other signaling proteins expressed in astrocytes need to communicate with neurons to generate pain mediators. Previous reports found that CFA induces a delayed activation of spinal astroglia and a concomitant production and release of proinflammatory mediators that parallels the pain behaviors in the later phases of peripheral inflammation [5;24;37]. The proinflammatory cytokine, IL-1β has been implicated in the maintenance of persistent pain states [25]. We did not observe IL-1β expression in the SCDH in the absence of CFA. However, in both vector control and NR1 KO mice, IL-1β expression was modestly increased in the SCDH at 24 hr but significantly increased at 96 hr after CFA. This expression of IL-1β was colocalized with GFAP and therefore in astrocytes, but not in neurons or microglia. Most studies of CFA-induced inflammation have not found significant microglia activation [4;21;22].

If IL-1β contributes to the late or NMDAR-independent maintenance phase of inflammatory pain hypersensitivity at 96 hr after CFA, then its expression should be limited in the ERK2 KD that provides persistent protection from CFA-induced allodynia. Indeed, we found that the CFA-induced increase in IL-1β in the SCDH at 96 hr after CFA was completely blocked in the ERK2 KD. We then examined the ability of the IL-1 receptor antagonist (IL-1ra) to reverse

inflammatory allodynia in our models. Pretreatment with intrathecal IL-1ra prevents inflammatory pain behaviors in animals [20;32;37]. In a more clinically relevant model, we examined the effect of IL-1ra to reverse inflammatory allodynia when administered after CFA. In contrast to our results with either the NR1 KO or the NMDAR antagonist, a single intrathecal dose of IL-1ra at 96 hr after CFA completely reversed the inflammation–induced allodynia in both the vector control and NR1 KO mice. We did not examine the antiallodynic efficacy if IL-1ra at earlier time points.

The receptors for glial cytokines are expressed by neurons [31;37], and this report (supplemental Fig. 2)), and cytokines like IL-1β facilitate the maintenance of injury-induced pain [10]. One consequence of the activation of neurons by IL-1β is the induction of neuronal PKCγ [10;27], which we found to be increased in both vector controls and NR1 KO at 96 hr after CFA (data not shown).

In this report we did not attempt to examine many of the other signaling candidates that may be activated in parallel with pERK2 or pPKCγ [15]. However, we do provide convergent data that suggests the activation of these kinases and the cytokine, IL-1β, play a prominent role in the early induction and later maintenance phases of inflammatory allodynia. Our studies identify critical players and provide important tools for future investigation of the downstream neuronal mediators of inflammatory pain.

In sum, we have identified important components of a feed forward signaling cascade that appears to be responsible for the early and maintenance phases of inflammatory allodynia following intraplantar CFA. Deletion of NMDAR-dependent signaling in neurons protects against early CFA-induced allodynia. Subsequent NMDAR-independent signaling that involves neuronal expression of pPKCγ and the induction of pERK2 and IL-1β in activated astrocytes contributes to the emergence of NMDAR-independent inflammatory pain behavior at 96 hr after CFA. These results may explain the limited clinical utility of NMDAR antagonists for injury-induced pain since the maintenance of these pain states appears with time after injury to become independent of NMDAR mediation. Further, they suggest that effective reduction of inflammatory pain requires targeting the neuron-astrocyte-IL-1β interactions revealed in these studies.

Supplementary Material

Refer to Web version on PubMed Central for supplementary material.

Acknowledgments

We thank Drs. H.T. Cheng, Ann Gregus and Deborah M. Hegarty for advice and/or assistance. These studies were supported in part by NIDA grants DA001457, DA000198, NIDA center grant DA005130 (CEI) and NIDA training grant DA007274 (ARW). We thank Amgen (Thousand Oaks, CA) for their gift of IL-1ra and placebo and Eli Lilly (Indianapolis, IN) for their gift of LY235959.

Q.X. and C.E.I. have submitted a patent application through Weill Cornell Medical College targeting ERK2 for pain management. No other potential conflicts of interest.

References

1. Cao H, Zhang YQ. Spinal glial activation contributes to pathological pain states. Neurosci Biobehav Rev 2008;32:972–983. [PubMed: 18471878]
2. Chaplan SR, Bach FW, Pogrel JW, Chung JM, Yaksh TL. Quantitative assessment of tactile allodynia in the rat paw. J Neuroscience Method 1994;53:55–63.

3. Cheng HT, Suzuki M, Hegarty DM, Xu Q, Weyerbacher AR, South SM, Ohata M, Inturrisi CE. Inflammatory pain-induced signaling events following a conditional deletion of the N-methyl-D-aspartate receptor in spinal cord dorsal horn. Neuroscience 2008;155:948–958. [PubMed: 18621103]
4. Clark AK, Gentry C, Bradbury EJ, McMahon SB, Malcangio M. Role of spinal microglia in rat models of peripheral nerve injury and inflammation. Eur J Pain 2007;11:223–230. [PubMed: 16545974]
5. Fu X, Zhu ZH, Wang YQ, Wu GC. Regulation of proinflammatory cytokines gene expression by nociceptin/orphanin FQ in the spinal cord and the cultured astrocytes. Neuroscience 2007;144:275–285. [PubMed: 17069983]
6. Garraway SM, Xu Q, Inturrisi CE. Design and Evaluation of Small Interfering RNAs That Target Expression of the N-Methyl-D-aspartate Receptor NR1 Subunit Gene in the Spinal Cord Dorsal Horn. J Pharmacol Exp Ther 2007;322:982–988. [PubMed: 17551091]
7. Garraway SM, Xu Q, Inturrisi CE. siRNA-mediated knockdown of the NR1 subunit gene of the NMDA receptor attenuates formalin-induced pain behaviors in adult rats. J Pain 2009;10:380–390. [PubMed: 19185544]
8. Giles PA, Trezise DJ, King AE. Differential activation of protein kinases in the dorsal horn in vitro of normal and inflamed rats by group I metabotropic glutamate receptor subtypes. Neuropharmacology 2007;53:58–70. [PubMed: 17543352]
9. Gillis JC, Benfield P, Goa KL. Transnasal butorphanol. A review of its pharmacodynamic and pharmacokinetic properties, and therapeutic potential in acute pain management. Drugs 1995;50:157–175. [PubMed: 7588085]
10. Guo W, Wang H, Watanabe M, Shimizu K, Zou S, LaGraize SC, Wei F, Dubner R, Ren K. Glial-cytokine-neuronal interactions underlying the mechanisms of persistent pain. J Neurosci 2007;27:6006–6018. [PubMed: 17537972]
11. Hu HJ, Carrasquillo Y, Karim F, Jung WE, Nerbonne JM, Schwarz TL, Gereau RWt. The kv4.2 potassium channel subunit is required for pain plasticity. Neuron 2006;50:89–100. [PubMed: 16600858]
12. Hylden JL, Wilcox GL. Intrathecal morphine in mice: a new technique. Eur J Pharmacol 1980;67:313–316. [PubMed: 6893963]
13. Ji RR, Baba H, Brenner GJ, Woolf CJ. Nociceptive-specific activation of ERK in spinal neurons contributes to pain hypersensitivity. Nature 1999;2:1114–1119.
14. Ji RR, Befort K, Brenner GJ, Woolf CJ. ERK MAP kinase activation in superficial spinal cord neurons induces prodynorphin and NK-1 upregulation and contributes to persistent inflammatory pain hypersensitivity. J Neurosci 2002;22:478–485. [PubMed: 11784793]
15. Ji RR, Gereau RWt, Malcangio M, Strichartz GR. MAP kinase and pain. Brain Res Rev. 2008
16. Ji RR, Kohno T, Moore KA, Woolf CJ. Central sensitization and LTP: do pain and memory share similar mechanisms? Trends Neurosci 2003;26:696–705. [PubMed: 14624855]
17. Kaspar BK, Vissel B, Bengoechea T, Crone S, Randolph-Moore L, Muller R, Brandon EP, Schaffer D, Verma IM, Lee KF, Heinemann SF, Gage FH. Adeno-associated virus effectively mediates conditional gene modification in the brain. Proc Natl Acad Sci USA 2002;99:2320–2325. [PubMed: 11842206]
18. Kawasaki Y, Kohno T, Zhuang ZY, Brenner GJ, Wang H, Van Der Meer C, Befort K, Woolf CJ, Ji RR. Ionotropic and metabotropic receptors, protein kinase A, protein kinase C, and Src contribute to C-fiber-induced ERK activation and cAMP response element-binding protein phosphorylation in dorsal horn neurons, leading to central sensitization. J Neurosci 2004;24:8310–8321. [PubMed: 15385614]
19. Kohno T, Wang H, Amaya F, Brenner GJ, Cheng JK, Ji RR, Woolf CJ. Bradykinin enhances AMPA and NMDA receptor activity in spinal cord dorsal horn neurons by activating multiple kinases to produce pain hypersensitivity. J Neurosci 2008;28:4533–4540. [PubMed: 18434532]
20. Laughlin TM, Bethea JR, Yezierski RP, Wilcox GL. Cytokine involvement in dynorphin-induced allodynia. Pain 2000;84:159–167. [PubMed: 10666520]
21. Lin T, Li K, Zhang FY, Zhang ZK, Light AR, Fu KY. Dissociation of spinal microglia morphological activation and peripheral inflammation in inflammatory pain models. J Neuroimmunol 2007;192:40–48. [PubMed: 17919739]

22. Lindia JA, McGowan E, Jochnowitz N, Abbadie C. Induction of CX3CL1 expression in astrocytes and CX3CR1 in microglia in the spinal cord of a rat model of neuropathic pain. J Pain 2005;6:434–438. [PubMed: 15993821]

23. Mandell JW, VandenBerg SR. ERK/MAP kinase is chronically activated in human reactive astrocytes. Neuroreport 1999;10:3567–3572. [PubMed: 10619645]

24. Menetski J, Mistry S, Lu M, Mudgett JS, Ransohoff RM, Demartino JA, Macintyre DE, Abbadie C. Mice overexpressing chemokine ligand 2 (CCL2) in astrocytes display enhanced nociceptive responses. Neuroscience 2007;149:706–714. [PubMed: 17870246]

25. Milligan ED, Watkins LR. Pathological and protective roles of glia in chronic pain. Nat Rev Neurosci 2009;10:23–36. [PubMed: 19096368]

26. Miyabe T, Miletic V. Multiple kinase pathways mediate the early sciatic ligation-associated activation of CREB in the rat spinal dorsal horn. Neurosci Lett 2005;381:80–85. [PubMed: 15882794]

27. Obreja O, Rathee PK, Lips KS, Distler C, Kress M. IL-1 beta potentiates heat-activated currents in rat sensory neurons: involvement of IL-1RI, tyrosine kinase, and protein kinase C. FASEB J 2002;16:1497–1503. [PubMed: 12374772]

28. Shimoyama N, Shimoyama M, Davis AM, Monaghan DT, Inturrisi CE. An Antisense Oligonucleotide to the N-Methyl-D-aspartate (NMDA) Subunit NMDAR1 Attenuates NMDA-Induced Nociception, Hyperalgesia, and Morphine Tolerance. J Pharmacol Exp Ther 2005;312:834–840. [PubMed: 15388787]

29. South SM, Kohno T, Kaspar BK, Hegarty D, Vissel B, Drake CT, Ohata M, Jenab S, Sailer AW, Malkmus S, Masuyama T, Horner P, Bogulavsky J, Gage FH, Yaksh TL, Woolf CJ, Heinemann SF, Inturrisi CE. A conditional deletion of the NR1 subunit of the NMDA receptor in adult spinal cord dorsal horn reduces NMDA currents and injury-induced pain. J Neurosci 2003;23:5031–5040. [PubMed: 12832526]

30. Velazquez KT, Mohammad H, Sweitzer SM. Protein kinase C in pain: involvement of multiple isoforms. Pharmacol Res 2007;55:578–589. [PubMed: 17548207]

31. Wang XF, Huang LD, Yu PP, Hu JG, Yin L, Wang L, Xu XM, Lu PH. Upregulation of type I interleukin-1 receptor after traumatic spinal cord injury in adult rats. Acta Neuropathol 2006;111:220–228. [PubMed: 16456668]

32. Watkins LR, Martin D, Ulrich P, Tracey KJ, Maier SF. Evidence for the involvement of spinal cord glia in subcutaneous formalin induced hyperalgesia in the rat. Pain 1997;71:225–235. [PubMed: 9231865]

33. Wei F, Vadakkan KI, Toyoda H, Wu LJ, Zhao MG, Xu H, Shum FW, Jia YH, Zhuo M. Calcium calmodulin-stimulated adenylyl cyclases contribute to activation of extracellular signal-regulated kinase in spinal dorsal horn neurons in adult rats and mice. J Neurosci 2006;26:851–861. [PubMed: 16421305]

34. Woolf CJ, Costigan M. Transcriptional and posttranslational plasticity and the generation of inflammatory pain. Proc Natl Acad Sci USA 1999;96:7723–7730. [PubMed: 10393888]

35. Woolf CJ, Salter MW. Neuronal plasticity: increasing the gain in pain. Science 2000;288:1765–1769. [PubMed: 10846153]

36. Xu Q, Garraway SM, Weyerbacher AR, Shin SJ, Inturrisi CE. Activation of the neuronal extracellular signal-regulated kinase 2 in the spinal cord dorsal horn is required for complete Freund's adjuvant-induced pain hypersensitivity. J Neurosci 2008;28:14087–14096. [PubMed: 19109491]

37. Zhang RX, Li A, Liu B, Wang L, Ren K, Zhang H, Berman BM, Lao L. IL-1ra alleviates inflammatory hyperalgesia through preventing phosphorylation of NMDA receptor NR-1 subunit in rats. Pain 2008;135:232–239. [PubMed: 17689191]

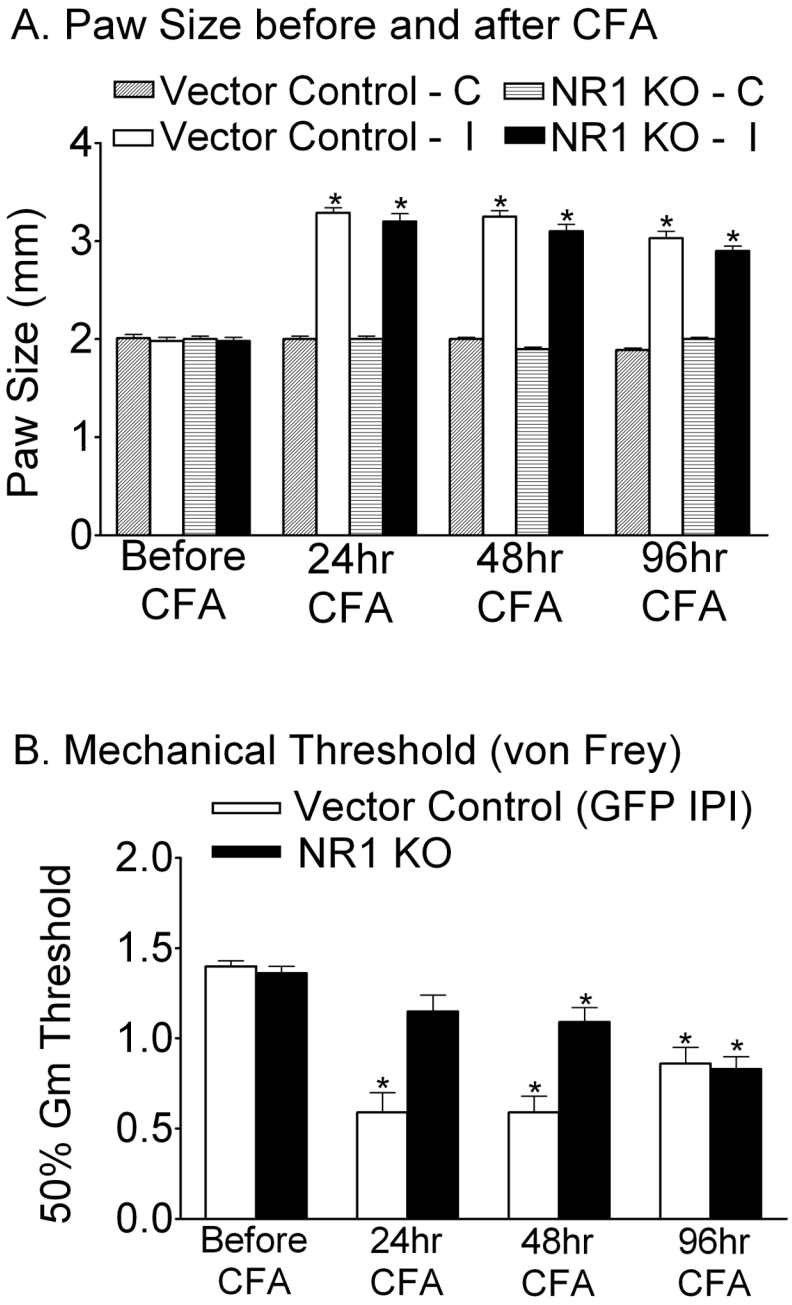

Fig. 1.

A spatial (spatiotemporal) knockout of the NR1 gene (NR1 KO) resulting from the intraparenchymal injection (IPI) of rAAV-GFP-Cre into the SCDH of a floxed NR1 (fNR1) mouse significantly reduces mechanical allodynia caused by the intraplantar injection of the inflammatory agent, complete Freund's adjuvant (CFA) at 24 and 48 hr, but not 96 hr after CFA treatment. Vector Control mice received the rAAV-GFP vector by IPI. **A**, CFA resulted in equivalent inflammation in the right (ipsilateral) (**I**) paw in both Vector Control and NR1 KO mice as measured by paw size at 24, 48 and 96 hr (*$p<0.05$, vs. baseline, n=16 per treatment group). The left (contralateral) (**C**) paw size was not affected. **B**, Mice that received the Vector Control by IPI exhibited mechanical allodynia as measured by a reduction in the mechanical

threshold (50% Gm threshold) using von Frey hairs applied to the ipsilateral paw at 24, 48 and 96 hr after intraplantar CFA compared to the baseline (*p< 0.05, vs. baseline). NR1 KO mice were protected from CFA-induced mechanical allodynia (**B**) at 24 and 48 hr, but not at 96 hr after CFA treatment (*p<0.05, vs. baseline, n=16 per treatment group). Error bars indicate SEM.

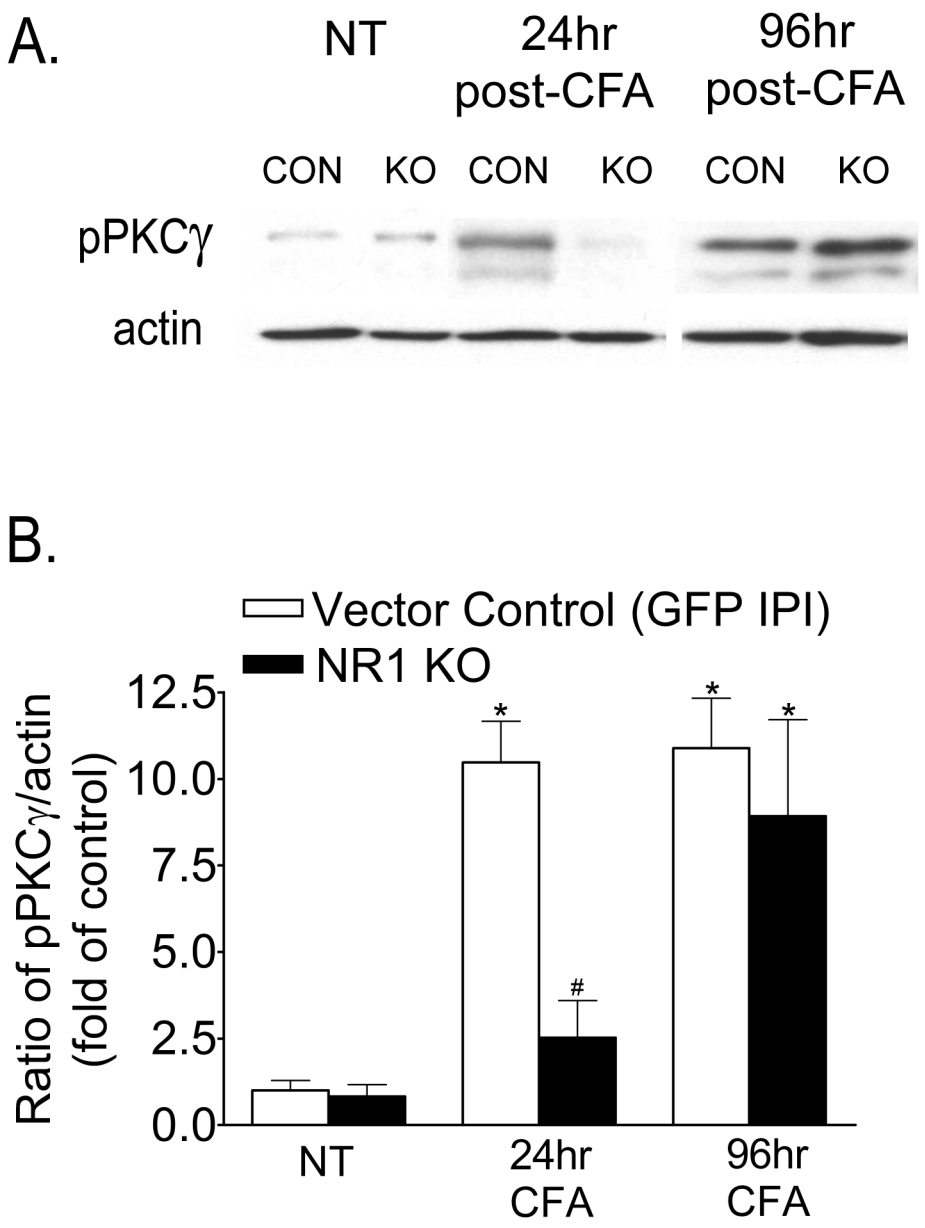

Fig. 2.

A spatial knockout of NR1 in the ipsilateral SCDH attenuates the expression of phospho-PKCγ (pPKCγ) in the lumbar spinal cord induced by intraplantar CFA at 24 h, but not at 96 hr after CFA treatment. An example of the Western blot is shown in **A** and the relative protein levels of pPKCγ are shown in **B. A, B**, Western blot analysis shows that pPKCγ was significantly increased in the ipsilateral spinal cord at 24 and 96 hr after intraplantar CFA in mice that received the Vector Control by IPI compared to the ipsilateral spinal cord of Vector Control or NR1 KO mice that did not receive CFA (No Treatment, NT) (*$p<0.05$ vs NT). pPKCγ is not significantly increased in the ipsilateral spinal cord of NR1 KO mice at 24 hr after intraplantar CFA compared to the ipsilateral spinal cord of Vector Control or NR1 KO mice that did not receive CFA (NT) (p value, 0.456). In contrast, pPKCγ expression is significantly increased in the ipsilateral spinal cord of both Vector Control and NR1 KO mice

at 96 hr after CFA (*p<0.05 vs corresponding NT). The data are the averages from three separate gel determinations. Error bars indicate SEM.

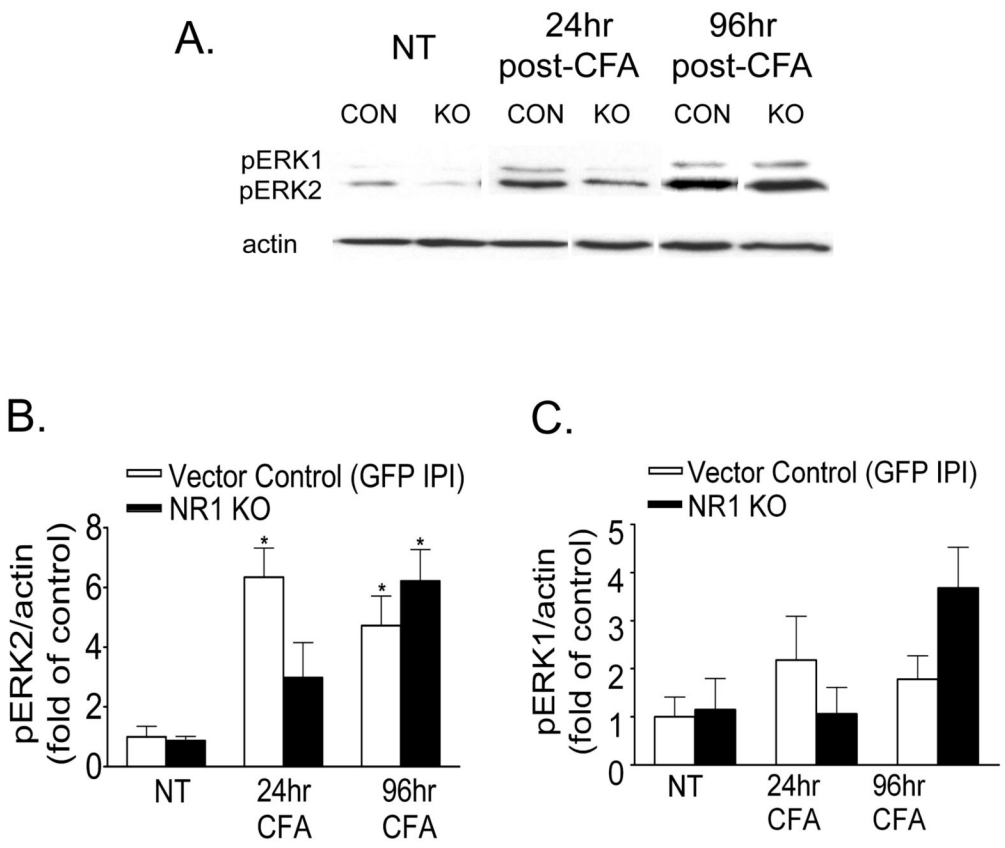

Fig. 3.

A spatial knockout of NR1 in the ipsilateral SCDH attenuates the expression of phospho-ERK2 (pERK2) in the lumbar spinal cord induced by intraplantar CFA at 24 hr, but not at 96 hr after CFA treatment. An example of the Western blot is shown in **A** and the relative protein levels of pERK2 and pERK1 are shown in **B** and **C. A, B**, Western blot analysis shows that pERK2 was significantly increased in the ipsilateral spinal cord at 24 and 96 hr after intraplantar CFA in mice that received the Vector Control by IPI compared to the ipsilateral spinal cord of Vector Control or NR1 KO mice that did not receive CFA (NT) (*$p<0.05$ vs NT). pERK2 expression is not significantly increased in the ipsilateral spinal cord of NR1 KO mice at 24 hr after intraplantar CFA compared to the ipsilateral spinal cord of Vector Control or NR1 KO mice that did not receive CFA (NT) (p value, 0.218). In contrast, pERK2 expression is significantly increased in the ipsilateral spinal cord of both Vector Control and NR1 KO mice at 96 hr after CFA (*$p<0.05$ vs corresponding NT). **A, C**, pERK1 expression in the ipsilateral spinal cord was not altered at 24 hr or 96 hr after CFA in mice that received the Vector Control or in NR1 KO mice (24 hr, p value 0.272; 96 hr, p value 0.087). The data are the averages from three separate gel determinations. Error bars indicate SEM.

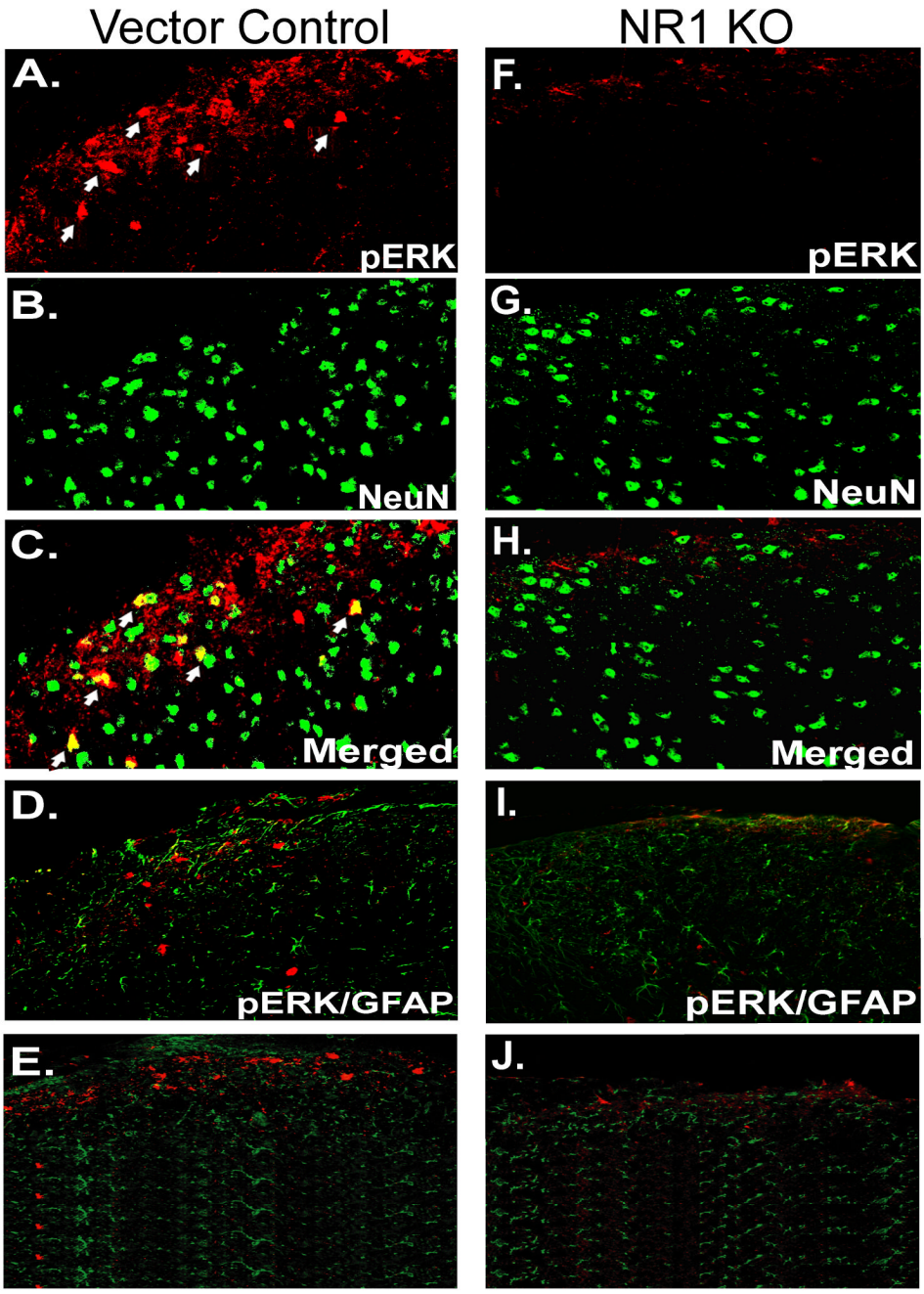

Fig. 4.

The expression of pERK1/2 by neurons (NeuN) is prevented in the ipsilateral SCDH of the NR1 KO at 24 h after intraplantar CFA. **A**, pERK1/2 immunolabeling was detected in the ipsilateral SCDH in Vector Control (red) at 24 hr after CFA. **B**, NeuN labeling revealed typically distributed neuronal morphologies (green). **C**-**E**, Merged image shows that pERK1/2 was colocalized with NeuN (**C**; yellow, arrows) but not GFAP (**D**) or OX42 (**E**) in the SCDH in Vector Control. **F**, pERK1/2 immunolabeling was attenuated in the SCDH in NR1 KO mice at 24 hr after CFA compared to mice that received the Vector Control by IPI (**A**). **G**, The NeuN labeling pattern is similar to that seen in the Vector Control sections (**B**). **H**, Merged image shows no colocalization of pERK1/2 and NeuN labeling in the SCDH of the NR1 KO compared

with Vector Control (**A**). **I-J**, pERK1/2 does not colocalize with GFAP (**I**) or OX42 (**J**) in the SCDH of the NR1 KO. Scale bar, 100 μm.

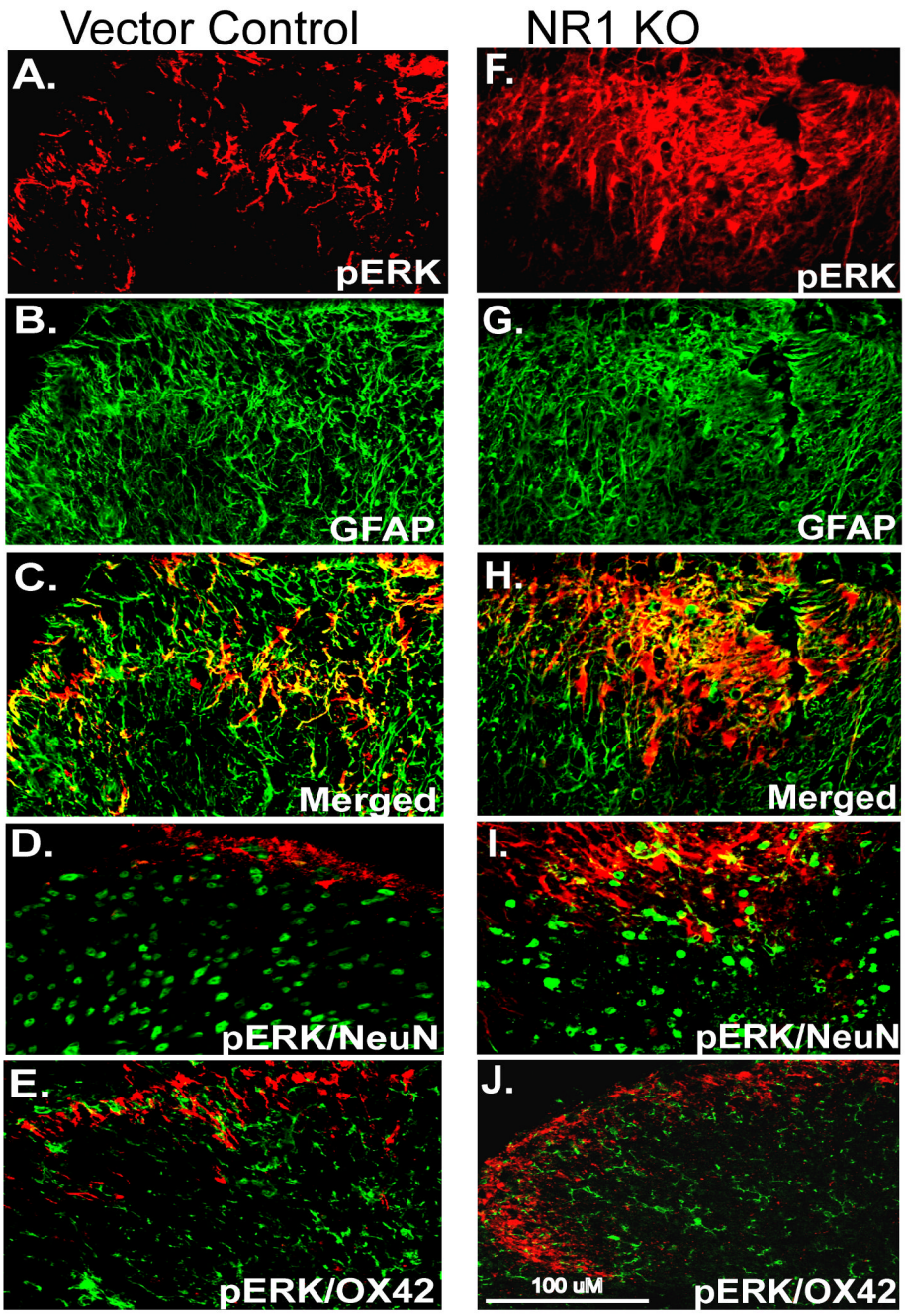

Fig. 5.

pERK1/2 colocalizes with GFAP in the ipsilateral SCDH of Vector Control and NR1 KO mice at 96 hr after intraplantar CFA. **A**, pERK1/2 immunolabeling was detected in the ipsilateral SCDH in mice that received the Vector Control by IPI (red). **B**, GFAP labeling revealed hypertrophy and thickening of processes (green), characteristic of reactive gliosis, in the Vector Control sections. **C-E**, Merged images show that pERK1/2 was colocalized with GFAP (**C**), but not with NeuN (**D**) or OX42 (**E**) in Vector Control sections. **F**, pERK1/2 immunolabeling was detected in the ipsilateral SCDH in NR1 KO mice. **G**, GFAP revealed morphological characteristics of active gliosis. **H-J**, Merged images show that pERK1/2 was colocalized with

GFAP (**H**), but not with NeuN (**I**) or OX42 (**J**) in the SCDH of NR1 KO mice. Scale bar, 100 μm.

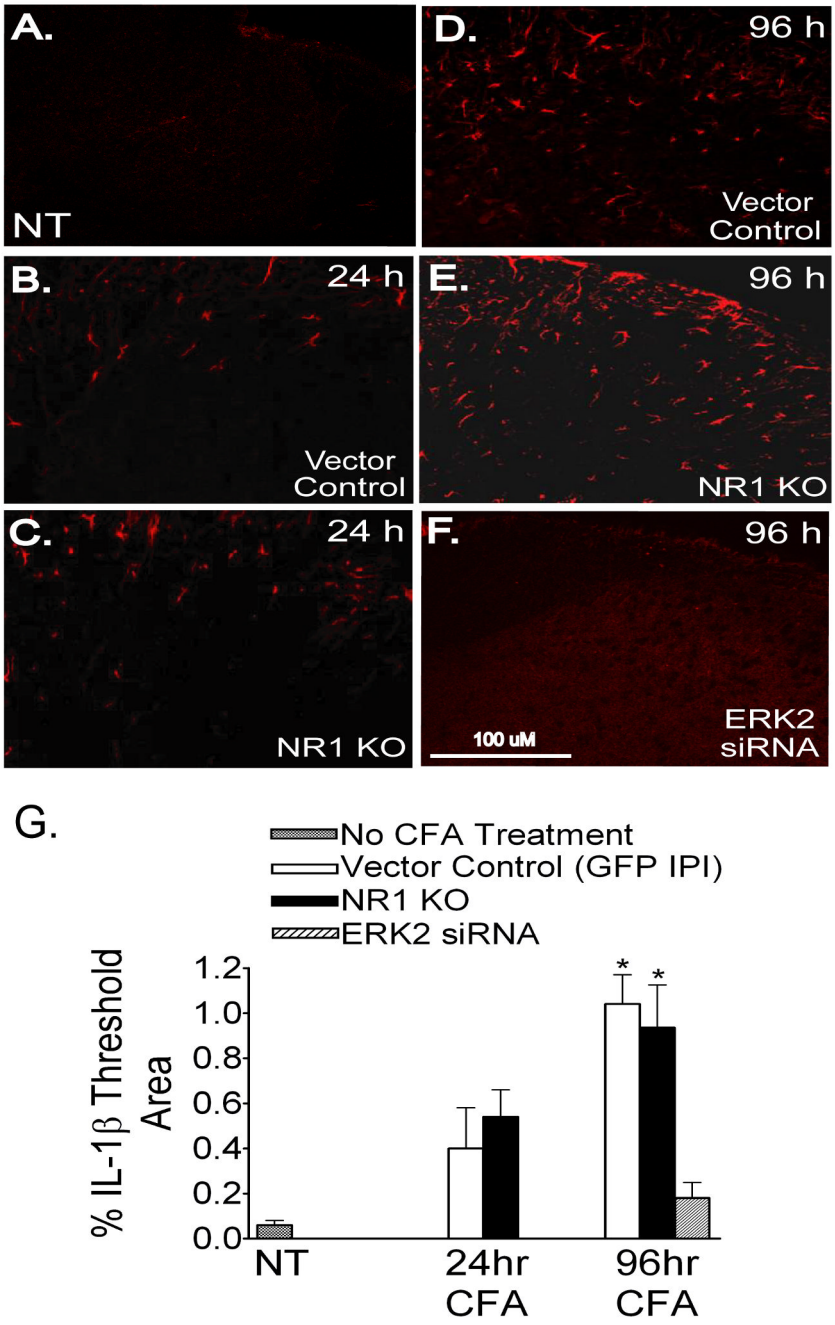

Fig. 6.

The expression of IL-1β is significantly increased in the ipsilateral SCDH of Vector Control and NR1 KO mice at 96 hr after intraplantar CFA. **A-F**, IL-1β immunolabeling in the SCDH (red). **G**, Quantification of IL-1β immunolabeling as percentage of threshold area in the SCDH. Data are mean ± SEM (n=3). **A**, IL-1β immunolabeling is absent from the SCDH of mice not treated with CFA (NT). **B-C**, At 24 hr after CFA, minimal IL-1β immunolabeling is present in the SCDH in Vector Control sections (**B**) and NR1 KO (**C**) sections which is not significantly different compared to mice not treated with CFA (NT) (**A**, see graph **G**) (p value, 0.108). **D-E,G**, At 96 hr after CFA, IL-1β immunolabeling is significantly increased in the SCDH in Vector Control (**D**) and NR1 KO sections (**E**) compared to mice that did not receive intraplantar

CFA (NT) and at 24 hr after CFA (see graph **G**) (*p<0.05 vs NT/24 hr). **F,G**, At 96 hr after CFA, IL-1β immunolabeling is absent in mice with a spatial knockdown of ERK2 in SCDH neurons as a result of the IPI of a rAAV vector expressing an ERK2 siRNA (**F** and graph, **G**). Scale bar, 100μm.

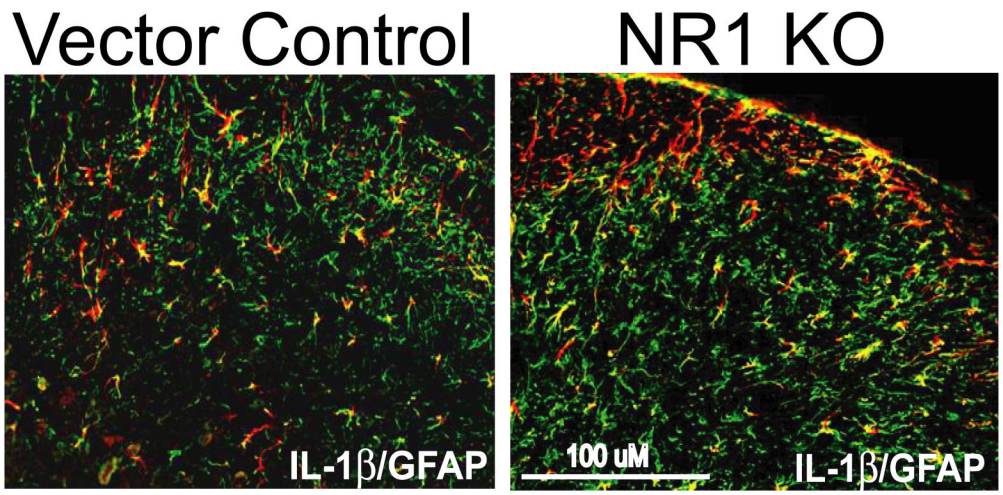

Fig. 7.

IL-1β colocalizes with GFAP in the ipsilateral SCDH of Vector Control and NR1 KO sections at 96 hr after intraplantar CFA. IL-1β (red) colocalizes with GFAP (green) in the SCDH in Vector Control and NR1 KO sections, Scale bar, 100μm.

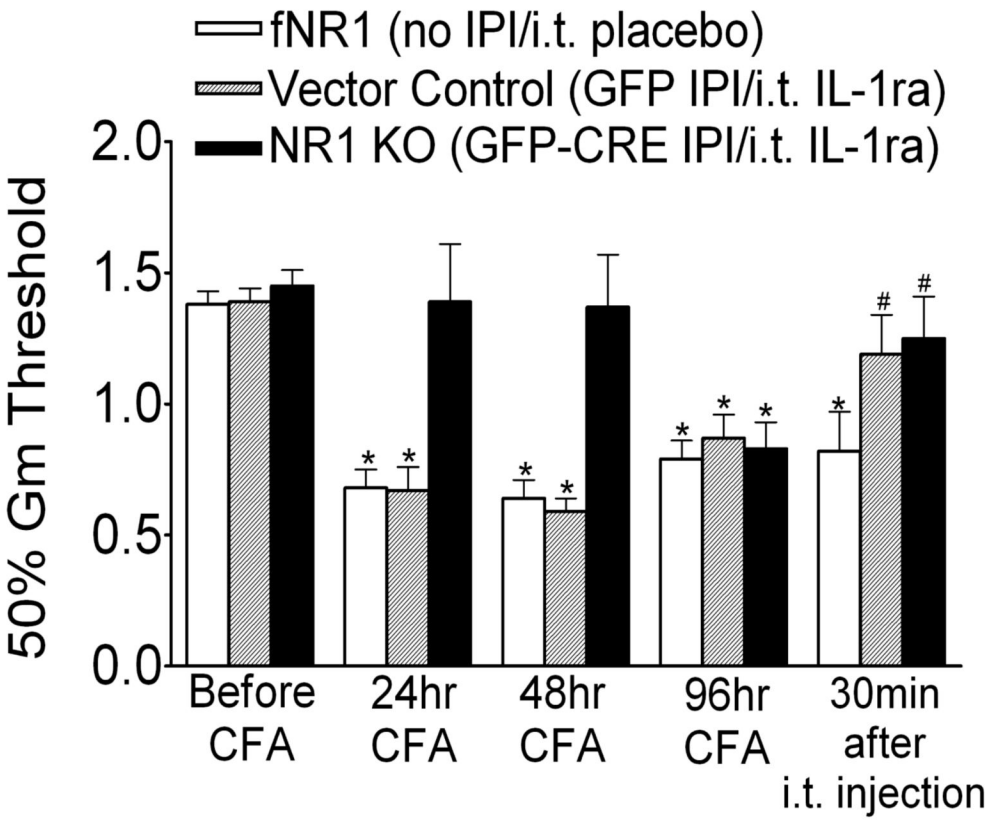

Fig. 8.

Intrathecal administration of the IL-1 receptor antagonist (IL-1ra) reverses the mechanical allodynia resulting from the intraplantar injection of CFA at 96 hr after intraplantar CFA. Mice with a floxed NR1 (fNR1) gene received either no IPI treatment, IPI with a rAAV vector expressing GFP (Vector Control) or IPI with a rAAV vector expressing GFP-Cre (NR1 KO). fNR1 and Vector Control mice showed mechanical allodynia as measured as a reduction in the mechanical threshold (50% Gm threshold) using von Frey hairs applied to the paw at 24, 48 and 96 hr after intraplantar CFA compared to the baseline (*$p < 0.05$, vs. baseline, n=10 per treatment group). NR1 KO mice were protected from CFA-induced mechanical allodynia at 24 and 48 hr, but not at 96 hr (n=14 per treatment group) after intraplantar CFA. Intrathecal (i.t.) administration of placebo drug in fNR1 mice at 96 hr after CFA did not affect CFA-induced mechanical allodynia (n=10 per treatment group). However, at 96 hr after CFA the i.t. administration of IL-1ra (10 μg/5 μl/mouse) reversed the mechanical allodynia at 30 min after IL-1ra in Vector Control and NR1 KO mice (#$p < 0.05$, vs. 96 hr).